Cross-Diffusion in a Water-in-Oil Microemulsion Loaded with Malonic Acid or Ferroin. Taylor Dispersion Method for Four-Component Systems

Vladimir K. Vanag, Federico Rossi,[†] Alexander Cherkashin,[‡] and Irving R. Epstein*

Department of Chemistry and Volen Center for Complex Systems, MS 015, Brandeis University, Waltham, Massachusetts 02454

Received: January 18, 2008; Revised Manuscript Received: April 14, 2008

We describe an improved Taylor dispersion method for four-component systems, which we apply to measure the main- and cross-diffusion coefficients in an Aerosol OT water-in-oil microemulsion loaded with one of the reactants of the Belousov−Zhabotinsky (BZ) reaction, water(1)/AOT(2)/R(3)/octane(4) system, where R is malonic acid or ferroin. With $[H_2O]/[AOT] = 11.8$ and volume droplet fraction $\varphi_d = 0.18$, when the microemulsion is below the percolation transition, the cross-diffusion coefficients D_{13} and D_{23} are large and positive ($D_{13}/D_{33} \cong 14$, $D_{23}/D_{33} \cong 3$) for malonic acid and large and negative for ferroin ($D_{13}/D_{33} \cong -112$, $D_{23}/D_{33} \cong -30$) while coefficients D_{31} and D_{32} are small and negative for malonic acid ($D_{31}/D_{33} \cong -0.01$, $D_{32}/D_{33} \cong -0.14$) and small and positive for ferroin ($D_{31}/D_{33} \cong 5 \times 10^{-4}$, $D_{32}/D_{33} \cong 8 \times 10^{-3}$). These data represent the first direct determination of cross-diffusion effects in a pattern-forming system and of the full matrix of diffusion coefficients for a four-component system. The results should provide a basis for modeling pattern formation in the BZ−AOT system.

1. Introduction

Understanding the mechanism of nonequilibrium pattern formation in dissipative physical, chemical, and biological systems is one of the most important challenges of nonlinear science. Most patterns in reaction−diffusion systems are thought to arise from either the Turing or the wave instability.[1] The Turing instability generates patterns that are stationary in space and time and possess an intrinsic wavelength. The wave instability (sometimes referred to as the finite wavelength instability) produces wavelike patterns, e.g., standing or packet waves, with a characteristic temporal period and spatial wavelength.

For two-variable systems, the Turing instability requires sufficiently different diffusion coefficients for the activator and inhibitor species, $D_{\text{inhibitor}} > D_{\text{activator}}$, a relationship often referred to as long-range inhibition and short-range activation. Localized stationary patterns can also emerge under this condition.[2,3]

The wave instability, which requires at least three variables, typically involves an additional fast-diffusing activator or a large diffusion coefficient for a third species that is coupled to the activator.[4–6] Both the Turing and wave instabilities generally require unequal self-diffusion (or intradiffusion) coefficients, i.e., the coefficients of proportionality between the flux of a species and its concentration gradient, with the single exception[7] of subcritical Turing instability under inhomogeneous initial conditions. On the other hand, there are several theoretical papers on systems with cross-diffusion,[8–12] whereby gradients in the concentration of one species affect the flux of another species, or with flow or convective terms,[13] which are analogous to cross-diffusion, that exhibit dissipative patterns even with equal self- or main-diffusion coefficients. Cross-diffusion terms are always present in biological chemotactic systems and are thought to be responsible for many patterns in bacterial colonies.[14–17]

An n-species reaction−diffusion system with cross-diffusion can be described by the partial differential equations

$$\frac{\partial c_i}{\partial t} = R_i(c_i, c_j) + \operatorname{div}(D_{ii} \nabla c_i) + \sum_{j \neq i} \operatorname{div}(D_{ij} \nabla c_j) \qquad (1)$$
$$i, j = 1, 2, \ldots, n$$

where the reactive, or chemical, term $R_i(c_i,c_j)$ depends in general on all the concentrations c_i; D_{ii} are the main-diffusion coefficients; and the cross-diffusion term, $\operatorname{div}(D_{ij}\nabla c_j)$, links the gradient of species c_j to the flux of species c_i. If $D_{ij} > 0$, then the ith species diffuses from larger to smaller concentrations of the jth species, analogous to the case of ordinary self-diffusion.[18] If $D_{ij} < 0$, then the ith species diffuses in the opposite direction, against the gradient ∇c_j. Unlike the main- (or diagonal) diffusion coefficients, D_{ii}, the cross-diffusion (or off-diagonal) coefficients D_{ij} must approach zero as c_i tends to zero, since there cannot be a flux of c_i if $c_i = 0$.

Finding a model that gives patterns similar to those observed experimentally is not sufficient to provide an understanding of reaction−diffusion systems, since quite different models can exhibit very similar patterns. To our knowledge, cross-diffusion coefficients have not previously been determined experimentally in any reaction−diffusion system that gives rise to pattern formation. The Belousov−Zhabotinsky reaction dispersed in Aerosol OT water-in-oil microemulsion (BZ−AOT system[19–21]) gives rise to perhaps the richest array of patterns of any reaction−diffusion system characterized to date. While we have been able to model most of these patterns using only self-diffusion terms, preliminary calculations suggest that the introduction of even small values of cross-diffusion coefficients can affect the system behavior dramatically.

Measurements of cross-diffusion coefficients in pure ternary AOT microemulsions (without BZ reactants) reveal that the

* Corresponding author. Phone: 781-736-2503. Fax: 781-736-2516. E-mail: epstein@brandeis.edu.

[†] Current address: Dipartimento di Chimica Fisica, Viale delle Scienze-Parco d'Orleans II - Edificio 17, 90128 Palermo, Italy.

[‡] Current address: Department of Biophysics, Faculty of Biology, Lomonosov Moscow State University, Moscow 119899, Russia.

10.1021/jp800525w CCC: $40.75
Published on Web 07/09/2008

cross-diffusion coefficient D_{12} (coefficient of proportionality between the flux of water induced by the gradient of [AOT] and the size of that gradient) can be significantly larger than both D_{11} and D_{22}.[22–24] The ratio D_{12}/D_{22} increases[26] with $\omega = [H_2O]/[AOT]$, which determines the mean radius r_w of the water droplets as[25] $r_w/\text{nm} \cong 0.17\omega$. At present, no data exist on cross-diffusion coefficients in quaternary systems composed of water, AOT, octane, and a single BZ reactant. There are several methods for measuring diffusion coefficients.[27] The Gouy or Rayleigh optical interferometry technique,[23,28,29] though highly accurate, is elaborate and subject to gravitational instabilities and convection (if one does not use a unique Gosting diffusiometer[30]) as well as being quite expensive to implement. The diaphragm-cell technique[31–33] is reliable and well-established, but it is extremely time consuming and is now rarely used. Pulsed NMR and dynamic light scattering are powerful methods for measuring self-diffusion coefficients (or, more precisely, the eigenvalues of the diffusion matrix **D**), but they have not been adapted to measuring cross-diffusion coefficients.

One of the most widely employed techniques for measuring main- and cross-diffusion coefficients is the Taylor method.[34–36] The Taylor dispersion technique is based on the diffusive spreading of a drop of solution injected into a laminarly flowing stream of the same mixture but with slightly different concentrations. A small volume of the perturbing solution is injected into the flowing eluent at the entrance of a long capillary tube. As it moves along the tube, the injected sample is deformed by the flow, the rate of which has a parabolic shape across the capillary, and by radial diffusion. The drop spreads out into a shape that can be fitted by a combination of n Gaussian functions for an $(n + 1)$-component system. The eluted peak, sometimes called the Taylor peak, is monitored by a suitable detector such as a flow-through spectrophotometer or a refractive index detector (RID). The diffusion coefficients are calculated from the parameters of the Gaussian functions that fit the eluted peak.

In three-component systems, there are direct relations between the fitting parameters (four parameters taken from the two Taylor peaks) and the four diffusion coefficients.[35] However, in quaternary systems there are no such relations for finding the nine diffusion coefficients. Usually, an experimentalist has six equations available to find nine unknown coefficients either in the Taylor method[37,38] or in the interferometry technique.[39,40] One procedure[38] employs simultaneous least-squares fitting of all experimental curves by a set of nine parameters. The precision of the least-squares fitting depends on the quality of the Taylor peaks. If the Taylor peaks can be unambiguously fitted by a set of three Gaussian curves, then the result of fitting procedure should be satisfactory. In most cases, however, the Taylor peaks can be satisfactorily fitted by more than one set of Gaussians, and it is difficult to choose the best fit. In some cases, the fitting procedure does not converge or it yields several local minima.[37] As a result, the error in some cross-diffusion coefficients can exceed 100%.[37]

To improve the results of fitting, a moment analysis procedure was developed.[37] In this method, three experimentally obtained values (combinations of the normalized peak height, and normalized first and second moments of dispersion profile) coupled by three linear equations are linearly linked to nine parameters that are combined to yield the nine diffusion coefficients. Although this method gives better results, the main drawback of the least-squares method remains, i.e., the uncertainty due to the existence of local minima.

In this paper, we introduce two new methods that directly link experimental data to the nine diffusion coefficients. In the first method, we employ the four ternary diffusion coefficients of the pure AOT microemulsion (obtained in additional experiments) that are assumed not to change significantly upon adding the fourth component (a reactant of the BZ reaction). This assumption is certainly not correct for a general four-component system,[29] but for AOT microemulsion loaded with a species, e.g., malonic acid, at relatively small concentration, it may be a reasonably accurate approximation. The second method employs data obtained from two different detectors, e.g., a refractive index detector and a flow-through spectrophotometer. This method is useful if a BZ reactant (ferroin in our case) has a large extinction coefficient in an accessible spectral range.

In section 2, we present the main ideas of the Taylor method for quaternary systems. In section 3 we develop the method for calculating diffusion coefficients from experimental data. Section 4 outlines the experimental procedures. As an illustration of our methods, we present in section 5 results on cross-diffusion coefficients in the water(1)/AOT(2)/malonic acid (or ferroin)(3)/octane system. We conclude with section 6. Derivations of many important formulas can be found in the Appendices and the Supporting Information.

2. Skeleton of the Theory. In this paper, we describe a Taylor dispersion method[34] for obtaining cross-diffusion coefficients in quaternary systems based in part on the ideas of Price,[35] who developed the Taylor method for three-component systems. We apply our technique to obtain the cross-diffusion coefficients of malonic acid, sodium malonate, and ferroin (reactants of the BZ reaction) in an AOT water-in-oil microemulsion.

The procedure is computationally complex, and we sketch here the general outline before presenting the details. In Table 1, we define a set of vectors and matrices used in the calculations. Our ultimate goal is to find the 3×3 diffusion matrix **D** for the full 4-component system. We do this by defining an effective diffusion matrix **F** for the radially averaged concentrations in the flow system, which can be inverted to yield **D**. By fitting the detector response observed when the injected droplet reaches the detector(s) to a sum of three Gaussians, we obtain a set of equations that relate the experimentally observed amplitudes and dispersions to the elements of **F**. It turns out that the maximal amount of information that can be derived from experiments with different droplet compositions yields only six independent equations for the nine elements of **F**. By utilizing data from experiments on the three component subsystem water/AOT/octane, we can find four of the elements of the diffusion matrix **D** and determine the remaining unknown elements of **D** using data for the quaternary system. In general, experiments on a three component subsystem provide four independent equations for the four elements of $\mathbf{D_2}$ or, equivalently, **E** (see Table 1). An alternative way to obtain three additional equations is to use data from a different detector, e.g., a spectrophotometer that is sensitive only to one component of the four-component system.

Consider a long, narrow, cylindrical tube with radius R_0 and impermeable walls, in which a homogeneous liquid mixture of four components flows under laminar conditions. The velocity profile for laminar flow in such a tube is parabolic:[34]

$$u(r) = 2u_0(1 - r^2) \tag{2}$$

where $r = R/R_0$, R is the radial distance from the tube axis, and u_0 is the mean velocity of the fluid mixture.

At time $t = 0$, a small drop containing the same four components, but with slightly different concentrations, is injected into the tube at axial coordinate $z = 0$ (z increases along the

TABLE 1: Vectors and Matrices Used in the Taylor Dispersion Method

	dimension	explanation
vectors		
φ	3, 4	volume fraction of component
c	2, 3	concentration of solute species, also used for concentration difference between flow and input concentrations
$\mathbf{c_0}$	2, 3	concentrations of injected species
P	2, 3	excess amount (in mol) of a component initially injected into flow, $P_i = V_0\Delta c_i$
G	2, 3	Gaussian fitting function (eq *13*)
σ	3	dispersion of Gaussian functions, eigenvalues of **F**
s	2	dispersion of Gaussian functions, eigenvalues of **E**
$\mathbf{P_{exp}}$	2, 3	experimental coefficients for fitting Taylor peaks
K	2, 3	sensitivity of detector signal to concentration of each species
matrices		
D	3 × 3	diffusion matrix for full system
$\mathbf{D_2}$	2 × 2	diffusion matrix for 3-component (water/AOT/octane) subsystem
F	3 × 3	effective diffusion matrix for flow system (eq. *9*)
E	2 × 2	effective diffusion matrix for 3-component subsystem (eq A3.1)
$\mathbf{M_Q}$	2 × 2	minor associated with element of matrix **Q**(**Q** = **D** or **F**)
B	3 × 3	coefficients for fitting concentration profiles with Gaussian functions for four component system (eq *12*)
A	2 × 2	coefficients for fitting concentration profiles with Gaussian functions for three-component system (eq *A3.9*)

flow direction). Since the volume of the sample introduced is small, we treat this injection as a δ-function perturbation. It is convenient to consider the evolution of the perturbation in a frame that moves along the z axis with velocity u_0. In this frame, the flow velocity $v(r)$ becomes

$$v(r) = u(r) - u_0 = u_0(1 - 2r^2) \tag{3}$$

The concentrations of the four components obey the relation:

$$\phi_1 + \phi_2 + \phi_3 + \phi_4 = 1 \tag{4}$$

where φ_i is the volume fraction of the ith component, and φ_i is related to the concentration c_i by

$$\phi_i = c_i M_i / d_i \tag{5}$$

where M_i is the molecular weight and d_i is the density of the ith component. Equation 4 implies that only three of the components are independent. We denote the concentration of the solvent (in our case, the oil, octane) as c_4 and write equations for the fluxes of the other three components in the moving frame for the z direction and for the radial direction:

$$J_{iz} = c_i u_0(1 - 2r^2) - \sum_{j=1}^{3} D_{ij}\frac{\partial c_j}{\partial z} \tag{6}$$

$$J_{iR} = -\sum_{j=1}^{3} D_{ij}\frac{\partial c_j}{\partial R} \tag{7}$$

$i = 1, 2, 3$. Using the continuity equation, we obtain three partial differential equations for our three independent species:

$$\frac{\partial c_i}{\partial t} = -\frac{\partial J_{iz}}{\partial z} - \frac{\partial J_{iR}}{\partial R} \tag{8}$$

Our first goal is to reduce eqs 8 to a simpler set of equations independent of R, taking the form

$$\frac{\partial c_i}{\partial t} = \sum_{j=1}^{3} F_{ij}\frac{\partial^2 c_j}{\partial z^2} \tag{9}$$

In Appendix 1, we show how to do this and find that

$$F_{ij} = \frac{R_0^2 u_0^2}{48\det(\mathbf{D})}\det(\mathbf{M}_{Dji})(-1)^{(i+j)} \tag{10}$$

where det(**D**) is the determinant of the 3 × 3 diffusion matrix **D** and det($\mathbf{M}_{Dji}$) is the determinant of the minor associated with element D_{ji} of **D**, for example, det($\mathbf{M}_{D21}$) = ($D_{12}D_{33} - D_{32}D_{13}$). The coefficients F_{ij} have the same dimensions as the diffusion coefficients D_{ij} (cm^2/s), but they are inversely proportional to D_{ij}. In the simplest case, when all the off-diagonal elements of **D** are zero, eq 10 reduces to $F_{ii} = K_{FD}/D_{ii}$, where $K_{FD} \equiv R_0^2 u_0^2/48$. Note that in eq 8 we consider c_i as a function of all three spatial coordinates, while in eq 9 c_i depends only on z, i.e., c_i in eq 9 is averaged over the cross section of the tube. One condition for the validity of the Taylor method is that measurements be made at "long times", at which the radial variation of c_i is small relative to the axial variation. Equations 9 have the same form as the equations for a one-dimensional diffusive process, and they can be solved analytically.

In the next section, we describe a procedure for finding the matrix **F** experimentally using the Taylor dispersion method. Knowing the elements of **F**, we can solve our main problem, i.e., finding the elements of **D,** by inverting eq 10:

$$D_{ij} = K_{FD}\det(\mathbf{M}_{Fji})(-1)^{(i+j)}/\det(\mathbf{F}) \tag{11}$$

where det($\mathbf{M}_{Fji}$) is the determinant of the minor associated with element F_{ji} of matrix **F**.

Matrices F and D. Equation 9 can be solved analytically. We note that eq 9 takes the same form for either the absolute concentrations c_i or the differential concentrations $\Delta c_i = c_{i0} - c_{i\_f}$, where c_{i_f} is the concentration in the flow solution and c_{i0} is the corresponding concentration in the injected sample. In the following we consider c_i as the differential concentration, omitting "Δ". We seek a solution of (9) of the form

$$c_i = \sum_{j=1}^{3} B_{ij}G_j \quad i = 1, 2, 3 \tag{12}$$

where G_i is the Gaussian function

$$G_i = \frac{1}{2\sqrt{\pi\sigma_i t}}\exp\left[-\frac{(z_0 - z)^2}{4\sigma_i t}\right] \quad i = 1, 2, 3 \tag{13}$$

Substituting eqs 12 and 13 into eq 9, we obtain

$$\sigma_j B_{ij} = \sum_{k=1}^{3} F_{ik}B_{kj} \;\; i = 1, 2, 3; j = 1, 2, 3 \tag{14}$$

from which it follows that the σ_i are the eigenvalues of **F**:

$$\begin{vmatrix} F_{11} - \sigma & F_{12} & F_{13} \\ F_{21} & F_{22} - \sigma & F_{23} \\ F_{31} & F_{32} & F_{33} - \sigma \end{vmatrix} = 0 \tag{15}$$

which also implies (Vieta's equations) that

$$\sigma_1 + \sigma_2 + \sigma_3 = F_{11} + F_{22} + F_{33} \tag{16}$$

$$\sigma_1\sigma_2 + \sigma_2\sigma_3 + \sigma_1\sigma_3 = \det(\mathbf{M}_{F11}) + \det(\mathbf{M}_{F22}) + \det(\mathbf{M}_{F33}) \tag{17}$$

$$\sigma_1\sigma_2\sigma_3 = \det(\mathbf{F}) \tag{18}$$

Therefore, only six of the nine equations in eq 14 are independent. To find the nine B_{ij} we must take into account three additional equations from the initial conditions for the three concentrations c_i:

$$P_i/(\pi R_0^2) = \sum_{j=1}^{3} B_{ij} \qquad i = 1, 2, 3 \tag{19}$$

where P_i is the excess (in mol) of the ith component injected at $t = 0$ and $z = 0$. We use this rather straightforward but cumbersome method of calculating B_{ij} from F_{ij} (see Supporting Information) for building the c_i through eq 12 and then reconstructing the signal S of our detector through eq 20 (see next paragraph). Comparing the reconstructed and experimentally found signals for different initial concentrations c_{i0} (or P_i) in the injected samples helps us to improve the reliability of the calculated coefficients D_{ij}, as we discuss in section 5.

Determining F_{ij} requires a detector that measures the dispersion (Taylor) peak at the end of our long narrow tube. When a refractive index detector is used, the signal S of the RID (measured in volts) is directly proportional to small changes in the concentrations of all the components of the flow mixture, i.e., to the c_i, and in the case of three independent concentrations (four components) can be fitted by a sum of three Gaussians:

$$S = \sum_{j=1}^{4} K_{jc} c_j = \sum_{i=1}^{3} P_{i,\mathrm{exp}} G_i \tag{20}$$

where the coefficients $P_{i,\mathrm{exp}}$ and the dispersions σ_i in G_i (eq 13) are found by fitting the experimental peaks. Using eqs 4 and 5, eq 20 can be rewritten as

$$\sum_{i=1}^{3} P_{i,\mathrm{exp}} G_i = \Delta\phi_1(K_{1c} d_1/M_1 - K_{4c} d_4/M_4) + \Delta\phi_2(K_{2c} d_2/M_2 - K_{4c} d_4/M_4) + \Delta\phi_3(K_{3c} d_3/M_3 - K_{4c} d_4/M_4) \tag{21}$$

Replacing $\Delta\varphi_i$ by $c_i M_i/d_i$, eq 21 transforms further to

$$\sum_{i=1}^{3} P_{i,\mathrm{exp}} G_i = \sum_{i=1}^{3} K_i c_i \tag{22}$$

where $K_i = K_{ic} - K_{4c} M_i d_4/(M_4 d_i)$, $i = 1, 2, 3$.

Using eq 12 and equating the coefficients of each of the G_i, we have

$$\sum_{j=1}^{3} K_j B_{ji} = P_{i,\mathrm{exp}} \quad i = 1, 2, 3 \tag{23}$$

Equations 14 and 19 enable us to replace the B_{ij} by the F_{ij} in eq 23. In Appendix 2, we derive the fundamental relations between the experimental data ($P_{i,\mathrm{exp}}$, σ_i) and the theoretical values (F_{ij}, K_1, K_2, K_3). Here, we simply write the final eqs 24 and 26 used for finding K_1, K_2, K_3, and finally the F_{ij}.

The general equation for the sensitivity coefficients K_i in eq 22 may be written as:

$$\left(\sum_{i=1}^{3} P_{i,\mathrm{exp}}\right)\pi R_0^2/V_0 = \sum_{i=1}^{3} K_i c_{i0} \tag{24}$$

where V_0 is the injected volume. By analyzing three experiments involving injections with only $c_{10} \neq 0$ or $c_{20} \neq 0$ or $c_{30} \neq 0$, we find from eq 24:

$$K_i = l_0^{-1}\left(\sum_{j=1}^{3} P_{j,\mathrm{exp\_}i}\right)/c_{i0} \quad i = 1, 2, 3 \tag{25}$$

where $l_0^{-1} = \pi R_0^2/V_0$ and $P_{j,\mathrm{exp\_}i}$ is the amplitude obtained for the j'th Gaussian by fitting the experiment in which only $c_{i0} \neq 0$. To find the F_{ij}, we employ the following fundamental relation:

$$l_0^{-1}\left(\sum_{j=1}^{3} \sigma_j P_{j,\mathrm{exp}}\right) = \sum_{i=1}^{3} c_{i0} \sum_{j=1}^{3} K_j F_{ji} \tag{26}$$

For the same three experiments with only $c_{10} \neq 0$ or $c_{20} \neq 0$ or $c_{30} \neq 0$ we have from eq 26:

$$\sum_{j=1}^{3} K_j F_{ji} = l_0^{-1}\left(\sum_{j=1}^{3} \sigma_j P_{j,\mathrm{exp\_}i}\right)/c_{i0} \equiv W_i \quad i = 1, 2, 3 \tag{27}$$

Equations 16–18 and eq 27 relate the F_{ij} to experimentally measurable quantities, but these six equations are insufficient to determine the nine F_{ij}. Additional experiments with initial injections having other compositions c_{i0} do not provide independent information, since the new equations, analogous to eq 26, are simply linear combinations of eq 27. Exactly this circumstance explains the relatively low precision of previous methods based on least-squares fitting. From a practical point of view, however, different combinations of the c_{i0} may make possible a more precise determination of the σ_i. To obtain enough equations to determine the F_{ij}, we must utilize additional information. If the fourth component cannot be detected spectrophotometrically and if this component does not affect significantly the interaction between the other three components (the structure of the AOT microemulsion in our case), then we may use the values of the cross- and main-diffusion coefficients found for a three-component subsystem under the assumption that these quantities remain unchanged on addition of the fourth component.

In Appendix 3, we summarize the key equations for the three-component system, including the equations analogous to our basic eqs 24 and 26. In the AOT microemulsion studied here, the natural choice for the three-component subsystem is water/AOT/octane, a system in which nanometer-size water droplets diffuse in the continuous oil (octane) phase. The fourth component can then be chosen as any of the reactants of the BZ reaction. We assume that the four diffusion coefficients of the pure AOT microemulsion (three-component system) remain nearly unchanged in the four-component system, e.g., when malonic acid or ferroin are added. We discuss the validity of this assumption in section 5.

We denote the components as water (1), AOT (2), and BZ reactant (3), with octane as the solvent. For the three-component system, we can measure D_{11}, D_{12}, D_{21}, and D_{22}, the main and cross-diffusion coefficients for water (1) and AOT (2). We define the matrix $\mathbf{D_2}$ with elements D_{11}, D_{12}, D_{21}, and D_{22}. The required additional equations for finding the F_{ij} can be obtained from eq 11, written for D_{11}, D_{12}, D_{21}, and D_{22}:

$$D_{11} = K_{FD}(F_{22}F_{33} - F_{23}F_{32})/(\sigma_1\sigma_2\sigma_3) \tag{28}$$

$$D_{22} = K_{FD}(F_{11}F_{33} - F_{13}F_{31})/(\sigma_1\sigma_2\sigma_3) \tag{29}$$

$$D_{12} = K_{FD}(F_{13}F_{32} - F_{12}F_{33})/(\sigma_1\sigma_2\sigma_3) \quad (30)$$

$$D_{21} = K_{FD}(F_{23}F_{31} - F_{21}F_{33})/(\sigma_1\sigma_2\sigma_3) \quad (31)$$

Equations 10 and 11 imply that

$$\det(\mathbf{F})\det(\mathbf{D}) = K_{FD}^3 \quad (32)$$

An analogous equation can be obtained for the matrices **E** and $\mathbf{D_2}$ for the three-component system (see Appendix 3):

$$\det(\mathbf{E})\det(\mathbf{D_2}) = K_{FD}^2 \quad (33)$$

The eigenvalues of **E**, s_1 and s_2, found experimentally for the three-component subsystem, are related by $s_1s_2 = \det(\mathbf{E})$; eq 18 gives $\sigma_1\sigma_2\sigma_3 = \det(\mathbf{F})$. Also, $\det(\mathbf{D_2}) = D_{11}D_{22} - D_{12}D_{21} = \det(\mathbf{M}_{D33})$, and eq 10 for F_{33} may be written as $F_{33} = K_{FD}\det(\mathbf{M}_{D33})/\det(\mathbf{D})$. These results can be combined with eqs 32 and 33 to yield

$$F_{33} = \sigma_1\sigma_2\sigma_3/s_1s_2 \quad (34)$$

Using eqs 17 and 28–31, we have

$$D_{11} + D_{22} + D_{33} = K_{FD}(1/\sigma_1 + 1/\sigma_2 + 1/\sigma_3) \quad (35)$$

An analogous expression can be written for the three-component system:

$$D_{11} + D_{22} = K_{FD}(1/s_1 + 1/s_2) \quad (36)$$

Combining eqs 35 and 36, we have

$$D_{33} = K_{FD}(1/\sigma_1 + 1/\sigma_2 + 1/\sigma_3 - 1/s_1 - 1/s_2) \quad (37)$$

Thus we can find F_{33} and D_{33} directly from the results of fitting the experimental peaks, independent of the other elements of **F** and **D**. There are many ways to obtain the remaining elements of **F** and **D** from the equations at our disposal. For example, from eqs 29, 31, and 27, we have

$$(\sigma_1\sigma_2\sigma_3)D_{22}/K_{FD} + F_{13}F_{31} = F_{11}F_{33} \quad (38)$$

$$-(\sigma_1\sigma_2\sigma_3)D_{21}/K_{FD} + F_{23}F_{31} = F_{21}F_{33} \quad (39)$$

$$K_1F_{11}F_{33} + K_2F_{21}F_{33} + K_3F_{31}F_{33} = W_1F_{33} \quad (40)$$

which can be combined to give

$$K_1(\sigma_1\sigma_2\sigma_3)D_{22}/K_{FD} - K_2(\sigma_1\sigma_2\sigma_3)D_{21}/K_{FD} + (K_1F_{13} + K_2F_{23})F_{31} + K_3F_{31}F_{33} = W_1F_{33} \quad (41)$$

Using eq 27 with $i = 3$, we finally obtain an expression for F_{31}

$$F_{31} = (K_{FD}W_1F_{33} + K_2D_{21}\sigma_1\sigma_2\sigma_3 - K_1D_{22}\sigma_1\sigma_2\sigma_3)/(K_{FD}W_3) \quad (42)$$

An equation for F_{32} can be found in the same fashion. Combining eqs 28, 30, and 27 gives

$$-K_1D_{12}(\sigma_1\sigma_2\sigma_3)/K_{FD} + K_2D_{11}(\sigma_1\sigma_2\sigma_3)/K_{FD} + (K_1F_{13} + K_2F_{23} + K_3F_{33})F_{32} = W_2F_{33} \quad (43)$$

Again using eq 27, we obtain

$$F_{32} = (K_{FD}W_2F_{33} + K_1D_{12}\sigma_1\sigma_2\sigma_3 - K_2D_{11}\sigma_1\sigma_2\sigma_3)/(K_{FD}W_3) \quad (44)$$

Utilizing eqs 10 and 11, eqs 42 and 44 give us equations for D_{31} and D_{32} in terms of the known F_{ij}:

$$D_{31} = -(D_{11}F_{31} + D_{21}F_{32})/F_{33} \quad (45)$$

$$D_{32} = -(D_{12}F_{31} + D_{22}F_{32})/F_{33} \quad (46)$$

Now only two elements of **D** remain to be found, namely D_{13} and D_{23}, along with the corresponding elements of **F**, F_{13} and F_{23}, as well as the elements F_{11}, F_{12}, F_{21}, and F_{22}, which differ from the elements E_{11}, E_{12}, E_{21}, and E_{22} of the three-component subsystem.

We can again use eqs 27–29 and the additional eq 16 to find F_{13} and F_{23}. Omitting some algebra, we finally obtain:

$$F_{13} = [F_{33}K_2(\sigma_1 + \sigma_2 + \sigma_3 - F_{33}) - K_2(1/s_1 + 1/s_2)\sigma_1\sigma_2\sigma_3 + (K_3F_{33} - W_3)F_{32}]/(K_2F_{31} - K_1F_{32}) \quad (47)$$

$$F_{23} = [F_{33}K_1(\sigma_1 + \sigma_2 + \sigma_3 - F_{33}) - K_1(1/s_1 + 1/s_2)\sigma_1\sigma_2\sigma_3 + (K_3F_{33} - W_3)F_{31}]/(K_1F_{32} - K_2F_{31}) \quad (48)$$

where the expressions for F_{31} and F_{32} in eqs 47 and 48 are taken from eqs 42 and 44, respectively. Knowing F_{13} and F_{23}, we can write equations for D_{13} and D_{23}:

$$D_{13} = -(D_{11}F_{13} + D_{12}F_{23})/F_{33} \quad (49)$$

$$D_{23} = -(D_{21}F_{13} + D_{22}F_{23})/F_{33} \quad (50)$$

Now, we know all the D_{ij} and can calculate F_{11}, F_{12}, F_{21}, and F_{22} using eq 10.

The equations for F_{11}, F_{12}, F_{21}, and F_{22} can be written as:

$$F_{11} = (D_{22}\sigma_1\sigma_2\sigma_3/K_{FD} + F_{13}F_{31})/F_{33} \quad (51)$$

$$F_{22} = \sigma_1 + \sigma_2 + \sigma_3 - F_{11} - F_{33} \quad (52)$$

$$F_{21} = (W_1 - K_1F_{11} - K_3F_{31})/K_2 \quad (53)$$

$$F_{12} = (W_2 - K_2F_{22} - K_3F_{32})/K_1 \quad (54)$$

The resulting values of D_{ij} are quite sensitive to the experimental data, σ_i, $P_{i,\mathrm{exp}}$, and W_i, as well as to the values of K_1, K_2, and K_3. Therefore independent determination of the D_{ij} is desirable if feasible.

If the detector is sensitive to only a single component, more accurate determination of diffusion coefficients D_{ij} is possible. For example, neither water nor AOT absorbs in the visible range. If we can detect component 3 optically, as in the case of ferroin, we can set $K_1 = K_2 = 0$ in eq 22 and simplify the subsequent equations. Equation 24, for example, takes the form

$$(P_{1,\mathrm{exp\_3}} + P_{2,\mathrm{exp\_3}} + P_{3,\mathrm{exp\_3}})\pi R_0^2/V_0 = K_3c_{30} \quad (24a)$$

and eqs 27 transform into

$$K_3F_{3i} = W_i \qquad i = 1, 2, 3 \quad (27a)$$

Equations 24a and 27a allow us to determine F_{3i} with greater accuracy, and eqs 45 and 46 can in turn be used to calculate D_{31} and D_{32}. In general, three eqs 27a obtained from optical detection, three eqs 27 obtained from refractive index detection, and three eqs 16–18 are sufficient to find all nine diffusion coefficients.

If it is possible to find another wavelength of light at which $K_2 = K_3 = 0$ (for example, in the IR), then eq 27 would yield more accurate expressions for the $F_{1i} = W_i/K_1$.

3. Experimental Section

Our experimental setup for the measurement of diffusion coefficients (see Supporting Information) is built around a high pressure liquid chromatography apparatus, which ensures suit-

able experimental conditions for the Taylor dispersion measurement.[36] The length of Teflon capillary tubing used in most experiments was about 30 m between the injector and the spectrophotometer cell (Shimadzu UV-1650PC) and 32 m between the injector and the cell of the differential flow-through refraction index detector, RID (Agilent 1100 series), though for some experiments we employed a 60 (62) m tube. The inner radius R_0 (= 0.42 mm) of the tubing was determined by gravimetry, i.e., from the mass of water required to fill the tube, and also by direct observation through a microscope of a thin slice of the tubing. The tubing was coiled in a 50 cm diameter helix. In experiments with malonic acid or sodium malonate, the Teflon capillary tubing is directly connected to the RID (the spectrophotometer was not used). An isocratic pump (Agilent G1310A), which maintained a steady flow, was placed between the eluent reservoir and the injector. Sample loops of volumes 10 and 20 μL were used for injection. Taylor peaks were detected at $\lambda = 510$ nm (ferroin molar extinction coefficient, $\epsilon_{510} = 1.1 \times 10^4$ $M^{-1}cm^{-1}$). The HPLC flow-thru cell (Shimadzu) has 1 mm internal diameter and path length $l_c = 1$ cm (8 μl inner volume). Both detectors were connected to a personal computer for data acquisition.

The eluent reservoir was also connected to a vacuum pump to degas the flowing solution. The injector and capillary tubing were kept at 23 °C in a thermostatted incubator (Fisher Scientific). All experiments with AOT microemulsions were run at a flow rate between 0.1 mL/min and 0.15 mL/min.

We also used a dynamic light scattering apparatus (DynaPro, Protein Solutions, High Wycombe, U.K.) to monitor the size of water droplets in the AOT microemulsion loaded with a reactant of the BZ reaction.

Water-in-oil microemulsions were prepared using bidistilled water, AOT (sodium bis(2-ethylhexyl)sulfosuccinate Aerosol OT, Aldrich) and octane (Sigma analytical grade). Octane was further purified by mixing with concentrated H_2SO_4 for two days; a stock solution of AOT in octane ([AOT] = 1.5 M) was prepared and filtered through a 0.45 μm Teflon filter to remove possible impurities.

The radius of the droplet of water core in nanometers is roughly given by $R_w = 0.17\omega$,[25,41,42] where $\omega = [H_2O]/[AOT]$; R_w is independent of the octane volume fraction in the microemulsion. The total radius of the droplet plus the surrounding AOT monolayer (hydrodynamic radius), R_d, exceeds R_w by the length of an AOT molecule (≈1.1 nm). Many physical properties of microemulsions show a threshold-like dependence on φ_d, the volume fraction of the dispersed phase ($\varphi_d = \varphi_{H_2O} + \varphi_{AOT}$). This dependence is due to percolation. If $\varphi_d \ll \varphi_{cr}$ (percolation threshold, $\varphi_{cr} \approx 0.5 - 0.6$), the microemulsion can be accurately characterized as a medium in which water droplets float freely.

Malonic acid (MA, Aldrich) and its disodium salt (Na_2MA, Fluka),were used as received. Ferroin was prepared by mixing 1,10-*o*-phenanthroline (Sigma) and $FeSO_4 \cdot 7H_2O$ (Fisher) in stoichiometric proportions (3:1) to get a 0.125 M stock solution. In the following, we specify concentrations of H_2O, AOT, MA, Na_2MA, ferroin, and octane with respect to the total volume of the microemulsion. Samples were injected every 3 h to avoid overlapping of the broad (up to 2 h wide) peaks. Experimental peaks generated with different injections were simultaneously fitted, using the Levenberg−Marquardt algorithm,[43] to the following equation:

$$v(t) = \sum_{i=1}^{3} \frac{P_{i,exp}}{\sqrt{4\pi\sigma_i t}} \exp\left[-\frac{u_0^2(t-t_0)^2}{4\sigma_i t}\right] \quad (55)$$

where $P_{i,exp}$, σ_i, and the retention time t_0 were chosen as fitting parameters. The expression $(z_0 - z)^2$ in eq (13) is replaced here by $u_0^2(t - t_0)^2$. A baseline of the form $(a + bt)$ was previously subtracted from the recorded signals with the help of suitable software.

4. Results

Two-Component Systems. In order to verify the condition of laminar flow, the flow rate was checked with a binary system of octane in hexane. Figure 1 shows that the diffusion coefficient is independent of eluent flow rate at $u_0 < 0.5$ mL/min. The value of D at the plateau (where $u_0 < 0.5$ mL/min), 3.4×10^{-5} cm^2/s, agrees well with earlier determinations.[44] At larger flow rates, turbulence apparently begins to affect diffusion in the tube. For a further check on the operation of the equipment, we measured the diffusion coefficient of an aqueous mannitol solution ($D = 0.656 \times 10^{-5}$ cm^2/s),[45] and the result was in agreement with the literature value to within the experimental error.

Water/AOT/Octane System. In order to calculate main- and cross-diffusion coefficients for the quaternary system, H_2O/AOT/BZ-reactant/octane, we determined the diffusivities in the ternary system, to which the fourth component (MA, Na_2MA, or ferroin) was later added. Microemulsions with several compositions below the percolation limit were investigated, and the results were used in our analysis of the quaternary system.

Several experiments were performed by injecting samples with an excess of one (H_2O or AOT) or two components. All Taylor dispersion peaks obtained were then simultaneously fitted using eq 55 with $i = 1, 2$ to extract the experimental parameters ($P_{i,exp}$, σ_i). Figure 2 shows the peaks obtained by injecting samples with an excess of only AOT (dashed line) or only H_2O (solid line) into a carrier stream of microemulsion with $\omega = 11.84$ and $\varphi_d = 0.18$. These peaks were used to calculate the instrumental sensitivity coefficients K_i using eq A3.11. We found that $K_1 = -2.07$ V/M and $K_2 = 42.3$ V/M. Note that these K_i are differences between K_{ic} and $K_{4c}M_id_4/(M_4d_i)$ (eq 22). Therefore, under some conditions, it is possible to obtain "negative" Taylor peaks.

Using eq A3.17 for E_{11} and eqs A3.12–A3.15, we found the E_{ij}, and then using eq A3.3, we transformed these results to diffusion coefficients D_{ij}. Then, using eqs A3.5–A3.8, we built analytical solutions of eq A3.1, the c_i given by eq A3.9, for many different injections and compared the analytical signals

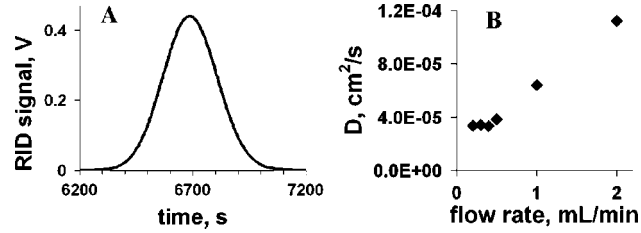

Figure 1. (A) Taylor dispersion profile for the 2-component system hexane-octane at $u_0 = 0.3$ mL/min (≅ 0.9022 cm/s for $R_0 = 0.042$ cm). The total length of capillary tubing used is $L_0 \cong 60$ m. The injected sample is octane; the eluent is hexane. The experimental curve is fitted by a single Gaussian with $P_{exp} = 119.65$ V × cm and $\sigma = 0.88$ cm^2/s. $D = R_0^2u_0^2/(48\sigma)$. (B) Dependence of the diffusion coefficient of octane in hexane on the average flow rate u_0 in the capillary. Error bars in (B) are smaller than the size of the symbols.

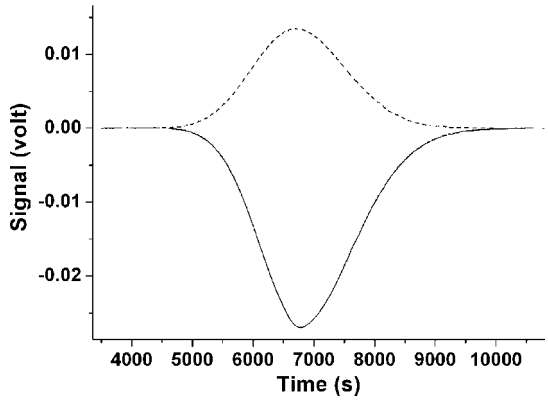

Figure 2. Taylor dispersion peaks for 3-component system water/AOT/octane. Injected samples contain an excess of AOT, $\Delta[AOT] = 0.075$ M, $\Delta[H_2O] = 0$ (dashed line) and an excess of H_2O, $\Delta[H_2O] = 3.108$ M, $\Delta[AOT] = 0$ (solid line). Composition of the carrier stream is $[H_2O] = 3.552$ M, [AOT] = 0.3 M, and [octane] = 5.046 M ($\omega = 11.84$ and $\varphi_d = 0.18$), $T = 23$ °C. Experimental peaks are fitted by a sum of two Gaussian curves with $P_{1,exp} = 3.51$ V × cm, $s_1 = 7.5$ cm²/s, $P_{2,exp} = 7.94$ V × cm, and $s_2 = 9.15$ cm²/s for dashed line and $P_{1,exp} = -4.78$ V × cm, $s_1 = 7.5$ cm²/s, $P_{2,exp} = -18.44$ V × cm, and $s_2 = 9.15$ cm²/s for solid line.

TABLE 2: Ternary Diffusion Coefficients and Sensitivity Coefficients K_i for Water (1) and AOT (2) in Water/AOT/Octane Microemulsions with $\omega = 11.84$ and $\varphi_d = 0.18$[a]

D_{11}	D_{12}	D_{21}	D_{22}	K_1	K_2
0.6 ± 0.04	7.8 ± 2	−0.01 ± 0.002	1.3 ± 0.04	−2.07	42.3

[a] Coefficients D_{ij} are reported in units of 10^{-6} cm²/sec, K_1 and K_2 in V/M.

(Taylor peaks) $S = K_1c_1 + K_2c_2$ to the corresponding experimental peaks. By tuning slightly the D_{ij} to minimize the difference between the analytical and corresponding experimental peaks, we were able to adjust all analytical peaks to the experimental ones. The resulting D_{ij} are reported in Table 2. The standard deviation associated with the fitting procedure itself is relatively small, but other factors, particularly the baseline subtraction, contribute larger sources of error. To estimate the uncertainty in our results, we can choose any two experimental peaks (like those shown in Figure 2) and find E_{ij} and then D_{ij}. Then we can replace one or two of the peaks with peaks obtained with different initial concentrations and find new values of E_{ij} and D_{ij}. From several sets of D_{ij} obtained in this fashion, we can obtain the mean $\langle D_{ij} \rangle$ and the corresponding standard deviations. The standard deviations found in this manner were typically in the range of 3−22%.

Water/AOT/MA/Octane and Water/AOT/Na_2MA/Octane Systems. Dynamic light scattering (DLS) experiments on the AOT microemulsion loaded with malonic acid or with Na_2MA (with concentrations as in our Taylor experiments) show a single narrow peak corresponding to the radius of the water droplets in pure AOT-ME (without additives). The coincidence of the radii for pure and loaded ME suggests that MA and Na_2MA probably have only a very small effect on the physical structure of the microemulsion, and consequently, it is reasonable to assume that the diffusion coefficients D_{11}, D_{12}, D_{21}, and D_{22} found for the ternary system are substantially unchanged in the quaternary system. The diffusion coefficient of water droplets, D_d, found in our DLS experiments is about 6.3×10^{-7} cm²/s for $\omega = 11.8$.

Figure 3 shows Taylor dispersion peaks generated by injection of samples in which the concentration of a single component

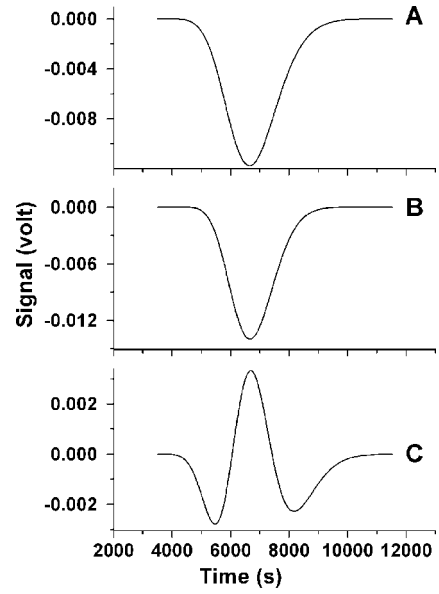

Figure 3. Taylor dispersion peaks for 4-component system water/AOT/MA/octane. Injected samples contain (A) an excess of H_2O, $\Delta[H_2O] = 1.5$ M, $\Delta[AOT] = \Delta[MA] = 0$, (B) a defect of AOT, $\Delta[AOT] = -0.075$ M, $\Delta[H_2O] = \Delta[MA] = 0$, and (C) an excess of MA, $\Delta[MA] = 0.032$ M, $\Delta[H_2O] = \Delta[AOT] = 0$. Composition of the carrier stream (eluent) is $[H_2O] = 3.552$ M, [AOT] = 0.3 M, [MA] = 0.032 M, [octane] = 5.046 M ($\omega = 11.84$, $\varphi_d = 0.18$), $T = 23$ °C.

TABLE 3: Preliminary Quaternary Diffusion Coefficients and Sensitivity Coefficients K_i for Water(1)/AOT(2)/MA(3)/Octane System at $\omega = 11.84$, $\varphi_d = 0.18$, [MA] = 0.032 M and $T = 23$ °C[a]

D_{13}	D_{23}	D_{31}	D_{32}	D_{33}	K_3
9.0	1.7	−0.004	−0.09	0.5	−12.3

[a] Coefficients D_{ij} are reported in units of 10^{-6} cm²/s, K_i in V/M. Coefficients D_{11}, D_{12}, D_{21}, D_{22}, K_1, and K_2 are the same as in Table 2.

differs from that in the carrier solution with $\omega = 11.84$, $\varphi_d = 0.18$, and [MA] = 0.032 M. The complex features of the peak in Figure 3C clearly show the presence of coupled flows associated with the diffusion of malonic acid. The peaks in Figure 3 allow us to calculate the sensitivity coefficients K_i, which are found to be substantially unchanged from the ternary system with the same ω and φ_d. This observation supports our assumption about the preservation of the major structural characteristics of the microemulsion upon addition of the fourth component.

The diffusion coefficients D_{11}, D_{12}, D_{21}, and D_{22} found in experiments with the ternary system, together with the experimental parameters ($P_{i,exp}$ and σ_i) extracted from the peaks in Figure 3, allowed us to calculate preliminary values of the F_{ij} and then the D_{ij}, the main- and cross-diffusion coefficients for the quaternary system H_2O/AOT/MA/octane. The results are summarized in Table 3.

The experimental peak in Figure 3C and the corresponding analytical solution constructed using the theoretical values of B_{ij} are shown in Figure 4. The contribution of each component c_i to the analytical peak is shown in the inset. The B_{ij} were numerically calculated from the equations given in the Supporting Information. Then theoretical signals were built (like those shown in Figure 5B−D) for the complete set of experimental peaks (Figure 5A). The best values for D_{ij} obtained by tuning the D_{ij} values in Tables 2 and 3 by a minimization procedure analogous to that applied above for the water/AOT/

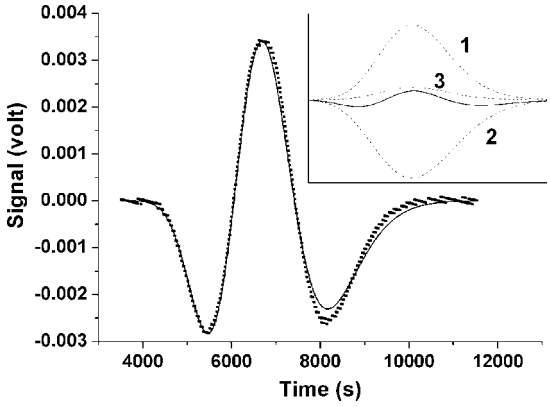

Figure 4. Comparison of the experimental Taylor peak (dotted line) shown in Figure 3C and the analytical solution (solid line) of the diffusion equation built with the calculated diffusion coefficients D_{ij}. Inset shows the composition of the analytical curve (solid line), i.e., the contribution of each component to the signal, and curves 1, 2, and 3 correspond to the signals of H_2O, AOT, and MA, respectively. Fitting parameters: $\sigma_1 = 7.97$ cm^2/s, $\sigma_2 = 12.4$ cm^2/s, $\sigma_3 = 8.1$ cm^2/s, $P_{1,\mathrm{exp}} = 25.5$ V × cm, $P_{2,\mathrm{exp}} = -21$ V × cm, $P_{3,\mathrm{exp}} = -6$ V × cm.

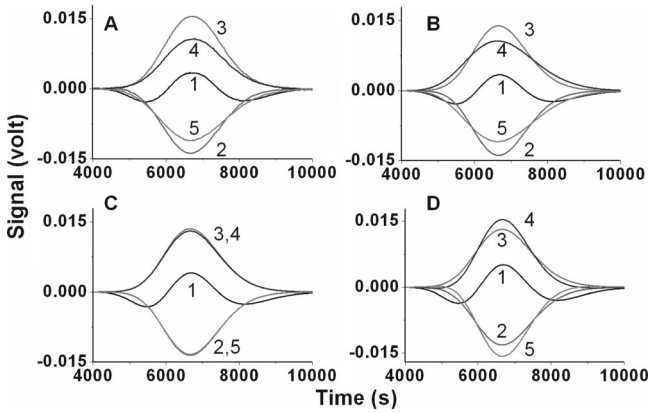

Figure 5. Experimental (A) and analytical (B–D) signals for 5 different samples in a carrier stream of the H_2O/AOT/MA/octane quaternary system ($\omega = 11.84$, $\varphi_d = 0.18$, [MA] = 0.032 M): (1) $\Delta[H_2O] = \Delta[AOT] = 0$, $\Delta[MA] = 0.032$ M; (2) $\Delta[H_2O] = 0$, $\Delta[AOT] = -0.075$ M, $\Delta[MA] = 0$; (3) $\Delta[H_2O] = 0$, $\Delta[AOT] = 0.075$ M, $\Delta[MA] = 0$; (4) $\Delta[H_2O] = -1.5$ M, $\Delta[AOT] = \Delta[MA] = 0$; and (5) $\Delta[H_2O] = 1.5$ M, $\Delta[AOT] = \Delta[MA] = 0$. (B) Best analytical signals used to calculate values in Table 3. (C) Analytical signals calculated with $D_{31} = D_{32} = 0$. (D) Analytical signals calculated with $D_{31} = 1 \times 10^{-9}$ cm^2/s and $D_{32} = 1 \times 10^{-8}$ cm^2/s.

TABLE 4: Quaternary Diffusion Coefficients (in cm²/s) for Water(1)/AOT(2)/MA(3)/Octane System at $\omega = 11.84$, $\varphi_d = 0.18$, [MA] = 0.032 M, and $T = 23$ °C[a]

j	D_{j1}	D_{j2}	D_{j3}
1	$(5.7 \pm 0.3) \times 10^{-7}$	$(6 \pm 2) \times 10^{-6}$	$(8 \pm 1) \times 10^{-6}$
2	$(-1.2 \pm 0.2) \times 10^{-8}$	$(1.6 \pm 0.3) \times 10^{-6}$	$(1.8 \pm 0.1) \times 10^{-6}$
3	$(-6 \pm 3) \times 10^{-9}$	$(-8 \pm 1) \times 10^{-8}$	$(5.6 \pm 0.7) \times 10^{-7}$

[a] Averaged values were found by tuning the D_{ij} in Tables II and III with the use of analytically obtained dispersion peaks.

octane subsystem are reported in Table 4. During this tuning procedure we constrained the eigenvalues of **D** to be real and positive, which necessitated small changes in the diffusion coefficients found previously. Comparison between the final values of D_{ij} in Table 4 and the preliminary values in Tables 2 and 3, as well as direct calculations of D_{ij} from different experimental curves, allow us to estimate the standard deviations for the D_{ij} presented in Table 4.

TABLE 5: Numerically Calculated Average Derivatives $\partial D_{ij}/\partial \sigma_i$ and Values of D_{ij}[a]

i, j	$\Delta D_{ij}/\Delta\sigma_1$	$\Delta D_{ij}/\Delta\sigma_2$	$\Delta D_{ij}/\Delta\sigma_3$	D_{ij}
1, 3	−1.5	0.36	−3	8.0
2, 3	0.005	0.06	0.07	1.8
3, 3	0.1	0.045	0.1	0.56
3, 2	0.015	−0.001	−0.0014	−0.08
3, 1	−0.0007	0.00012	0.00018	−0.006

[a] Coefficients D_{ij} are reported in units of 10^{-6} cm^2/s, $\Delta D_{ij}/\Delta\sigma_1$ in dimensionless units of 10^{-6}.

In addition to estimation of standard deviations, we also tested the robustness of our results by other methods. For example, we analyzed the effect on the analytical solution shown in Figure 5B of changes in the very small negative diffusion coefficients D_{31} and D_{32}. Panels C and D in Figure 5 report, respectively, the analytical solutions with $D_{31} = D_{32} = 0$ and with small positive values of D_{31} and D_{32}. Comparing Figure 5A with Figure 5C,D, it is evident that the curves in panels C and D in Figure. 5 deviate significantly from the corresponding experimental curves shown in Figure 5A.

Of course, this simple test is not sufficient to demonstrate the validity of the calculated diffusion coefficients. Concerted variations of several of the D_{ij} may lead to negligible changes in the analytical solutions. Such small concerted deviations can be generated by small changes in the fitting parameters σ_i and $P_{i,\mathrm{exp}}$. Analysis shows, however, that small variations in the σ_i and $P_{i,\mathrm{exp}}$ do not significantly affect the D_{ij}. We numerically calculated approximate values of the derivatives $\partial D_{ij}/\partial\sigma_i$ (see Table 5) by changing σ_i and calculating the resulting values of D_{ij}. Analogous values were obtained for $\partial D_{ij}/\partial P_{i,\mathrm{exp}}$ by varying $P_{i,\mathrm{exp}}$. The error in D_{ij} can be estimated as $(\partial D_{ij}/\partial\sigma_i)\Delta\sigma_i/D_{ij}$ or $(\partial D_{ij}/\partial P_{i,\mathrm{exp}})\Delta P_{i,\mathrm{exp}}/D_{ij}$, where $\Delta\sigma_i$ and $\Delta P_{i,\mathrm{exp}}$ are the errors in σ_i and $P_{i,\mathrm{exp}}$, respectively. We estimate $\Delta\sigma_i$ and $\Delta P_{i,\mathrm{exp}}$ to be 10−20% due to uncertainties in baseline subtraction and/or small errors in sample preparation, which cause slightly different values of K. These evaluations yield errors in the D_{ij} comparable to those shown in Table 4, i.e., 5−50% for the various D_{ij}. Such accuracy is more than sufficient for our ultimate purpose of modeling of dissipative patterns in the BZ−AOT system. We thus have some confidence that the D_{ij} obtained by this method are reasonably accurate.

A possible problem with the use of malonic acid as the fourth component may arise from the lack of a common ion between MA and AOT. Interdroplet collisions may cause an exchange between the hydrogen ions of malonic acid ($pK_{a1} = 2.83$, $pK_{a2} = 5.69$ in bulk water) and the sodium ions of AOT, generating a flux of the fifth component, making our system pseudoquaternary. The possibility of such a scenario is rather low, since dissociation of MA inside water droplets, where the dielectric constant ϵ is about 5−10 (instead of ≅ 80 in the bulk water),[46–48] should be small. Nevertheless this possibility is not zero, and we therefore investigated the contribution of these counterion fluxes (in the form of fluxes of Na_2MA or protonated AOT molecules, HSO_3−AOT) to our system by performing experiments with disodium malonate (Na_2MA) as the fourth component. The solubility of Na_2MA is smaller than that of MA, which resulted in the lower [Na_2MA] used in our experiments. The values of the main- and cross-diffusion coefficients (cf. Tables 4 and 6) are almost the same as in the case of malonic acid.

Comparing the diffusion coefficient of water droplets, D_d found in the DLS experiments ($D_d \cong 6.3 \times 10^{-7}$ cm^2/s) to the D_{ii} values found in the Taylor experiments, we see that D_d is very close to D_{11} and D_{33}.

TABLE 6: Quaternary Diffusion Coefficients (in cm²/s) for Water(1)/AOT(2)/Na_2MA(3)/Octane System at $\omega = 11.84$, $\varphi_d = 0.18$, $[Na_2MA] = 3.2 \times 10^{-3}$M, and T= 23°C[a]

j	D_{j1}	D_{j2}	D_{j3}
1	$(5.3 \pm 0.3) \times 10^{-7}$	$(4.9 \pm 2) \times 10^{-6}$	$(7 \pm 1) \times 10^{-6}$
2	$(-1.2 \pm 0.2) \times 10^{-8}$	$(1.5 \pm 0.3) \times 10^{-6}$	$(3 \pm 0.1) \times 10^{-6}$
3	$(-1.2 \pm 3) \times 10^{-9}$	$(-4 \pm 1) \times 10^{-8}$	$(5 \pm 0.7) \times 10^{-7}$

[a] Averaged values were found using the same procedure as for the system water(1)/AOT (2)/MA(3)/octane: $K_1 = -2.05$ V/M, $K_2 = 42.3$ V/M, and $K_3 = 47.2$ V/M.

Water/AOT/Ferroin/Octane system. Measurement of D_{ij} for this system is more complex. The problem is that the DLS spectrum has a second peak corresponding to a radius of about 20 nm. The larger the concentration of ferroin, the larger the amplitude of this peak, which probably indicates the presence of clusters of water droplets. To see clearly the RID signal corresponding to ferroin, its concentration in the injected solution must be relatively large; at such a concentration, the DLS spectrum is bimodal with two pronounced peaks. The use of a spectrophotometer as a second detector is very helpful in this situation.

Figure 6A−C shows the RID output for the Taylor dispersion peaks generated by the injection of samples in which the concentration of water, AOT, or ferroin, respectively, exceeds that in the carrier solution. The spectrophotometric peak corresponding to the RID peak in Figure 6C is shown in Figure 6D. The peak in Figure 6D is very well fitted by a single Gaussian curve, providing us with the dispersion of one of the three Gaussian functions, let say σ_3. Using eq 27a for $i = 3$ and the coefficient K_{3_spec} (K_{3_spec} coincides with the product $l_c\epsilon_{510}$, where ϵ_{510} is the extinction coefficient of ferroin at $\lambda = 510$ nm), we can calculate element F_{33} of the matrix **F**. Unfortunately, we were not able to use eq 27a to determine F_{31} and F_{32}, because the ferroin flux induced by the water and AOT gradients was too low to be detected spectrophotmetrically. Since the accuracy of our spectrophotometric detection is about 0.001 au (au = absorption units), the minimal detectable concentration of ferroin is about $0.001/(l_c\epsilon_{510}) \equiv 0.2\ \mu$M. Note that the minimal concentration of ferroin detectable by the RID and determined as V_{noise}/K_{3_RID} is also about 0.2 μM, since $V_{noise} \cong 0.1$ mV and $K_{3\_RID} \cong 500$ M/V (see Table 7).

Knowing σ_3, we can accurately determine the other two dispersions, σ_1 and σ_2, by fitting the peaks shown in Figures 6A−C. Knowing the value of F_{33} and the product $\sigma_1\sigma_2\sigma_3$, we can evaluate the product s_1s_2 using eq 34 and compare this value to the s_1s_2 found in pure AOT microemulsion (water/AOT/octane system). The good agreement between the two s_1s_2 values suggests that the diffusion coefficients D_{11}, D_{12}, D_{21}, and D_{22} do not change significantly in the quaternary system upon adding ferroin.

The shape of the peak in Figure 6C suggests the presence of coupled fluxes of water and AOT associated with the gradient of [ferroin]. Comparing the Taylor peaks in Figures 6C (for ferroin) and 3C (for malonic acid), we see that they lie in opposite directions. This fact is reflected in the opposite signs of all the cross-diffusion coefficients for ferroin and MA.

From our analysis of the Taylor peaks, we find that the values of K_1 and K_2 are the same as in the water/AOT/octane ternary system. Applying the same data analysis as employed for malonic acid, we obtain the main- and cross-diffusion coefficients reported in Table 7.

6. Discussion

In this paper, we have adapted the Taylor dispersion method to four-component systems by using data either from a three-component subsystem or from a second detector sensitive to the concentration of a single component. We showed that data from fitting the experimental Taylor peaks by three Gaussians can be transformed into the nine elements of the matrix **F** and then into the nine elements of the diffusion matrix **D** composed of the main- and cross-diffusion coefficients.

In principle, this theory can be extended to an arbitrary multicomponent system, which seems difficult, if not impossible, with previous methods.[37,38] In general, in an $(n + 1)$-component system with an $n \times n$ **D**-matrix, to find the n^2 elements of the corresponding **F**-matrix, we have n equations obtained from n independent RID-experiments with only $\Delta c_i \neq 0$ (cf. eq 25), n Vieta's equations (cf. eqs 16–18) relating the elements of **F** and the σ_i, and $(n - 1)^2$ elements of $\mathbf{D_{n-1}}$ from a suitable n-component subsystem measured in another set of experiments. The constraint $\det(\mathbf{F})\det(\mathbf{D}) = K_{FD}^n$ reduces the number of independent equations from $n + n + (n - 1)^2 = n^2 + 1$ to n^2. The eqs 24 and 26 generalize to

$$l_0^{-1}\sum_{i=1}^{n} P_{i\mathrm{exp}} = \sum_{i=1}^{n} K_i c_{i0} \tag{56}$$

$$l_0^{-1}\sum_{i=1}^{n} \sigma_i P_{i\mathrm{exp}} = \sum_{j=1}^{n} c_{j0} \sum_{i=1}^{n} K_i F_{ij} \tag{57}$$

For a three-component system, we can determine all four elements of $\mathbf{D_2}$ in just two experiments without performing experiments on a two-component subsystem. For more complex systems, however, beginning with the quaternary ($n = 4$) system, we have to perform experiments to determine the D_{ij} for an $(n - 1)$ component subsystem. This makes our theory matreshka-like. However, by using different detectors, e.g., an RID and a spectrophotometer (or Raman spectrometer[49]), it may be possible to find some of the D_{ij} directly from experiments only on the n-component system.

There are several potential pitfalls in our method. First, when we use coefficients D_{ij} found in an $(n - 1)$-component subsystem for determining D_{ij} in the n-component system, we must be sure that they are the same, i.e., that addition of the n^{th} component does not significantly alter the physical structure of the $(n - 1)$-component system or the interactions between these $(n - 1)$-components. In the case of AOT microemulsions, the fourth component can in general change the radius (or structure) of the water nanodroplets, if either the concentration or the linear extent of the fourth component is too large. We probably create such a situation when we use ferroin as the fourth component. One of the consequences of these changes might be the unusual shape of the Taylor peak shown in Figure 6C. This peak has two maxima, and the amplitude of the maximum at longer time is larger than the amplitude of the maximum at shorter time. This very reproducible shape cannot be well fitted by any combination of Gaussian curves with the same retention time t_0. At present, we do not have a satisfactory explanation for this phenomenon.

Second, in the case of AOT microemulsions, the sensitivity constant K_1 (for water) may depend on the radius of the water droplet core. This dependence originates from the dependence of the refractive index n on the dielectric permittivity and magnetic permeability, ϵ and μ, respectively:

$$n = (\varepsilon\mu/\varepsilon_0\mu_0) \tag{58}$$

where ϵ_0 and μ_0 are the values in vacuum, and in turn on the dependence of ϵ on ω (= $[H_2O]/[AOT]$).[46,47,50,51] In experiments

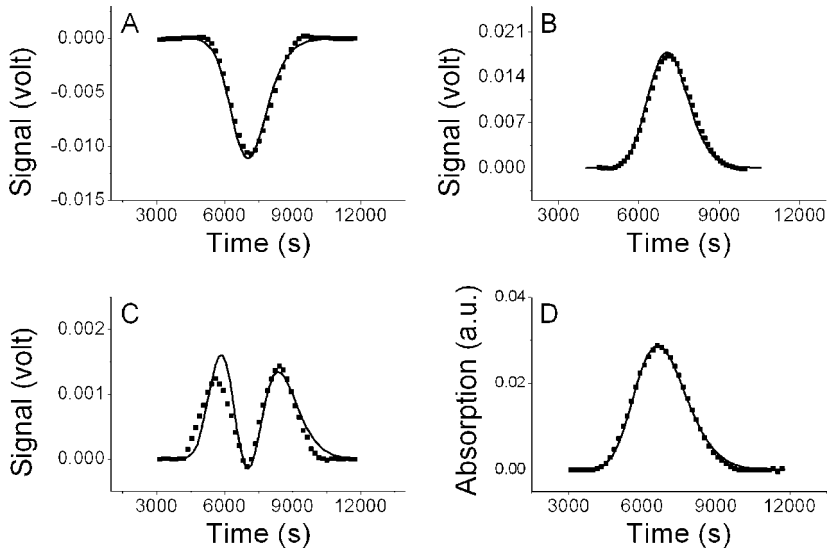

Figure 6. Taylor dispersion peaks for 4-component system water/AOT/ferroin/octane. (A−C) signals of RID and (D) absorption at $\lambda = 510$ nm (signal of spectrophotometer). Dotted lines show experimental peaks, and solid lines show analytical signals built using values from Table 7. Injected samples contain (A) an excess of H_2O, $\Delta[H_2O] = 1.5$ M, $\Delta[AOT] = \Delta[ferroin] = 0$; (B) an excess of AOT, $\Delta[AOT] = 0.1$ M, $\Delta[H_2O] = \Delta[ferroin] = 0$; and (C, D) an excess of Fe, $\Delta[Fe] = 1 \times 10^{-3}$ M, $\Delta[H_2O] = \Delta[AOT] = 0$. Composition of the carrier stream (eluent) is $[H_2O] = 3.552$ M, $[AOT] = 0.3$ M, $[ferroin] = 1.61 \times 10^{-5}$ M, [octane] = 5.046 M ($\omega = 11.84$, $\varphi_d = 0.18$), $T = 23$ °C. Fitting values of dispersions σ for all peaks: $\sigma_1 = 7.81$ cm²/s, $\sigma_2 = 8.51$ cm²/s, $\sigma_3 = 16.5$ cm²/s. (au = absorption units).

TABLE 7: Quaternary Diffusion Coefficients (in cm²/s) for Water(1)/AOT(2)/Ferroin(3)/Octane System at $\omega = 11.84$, $\varphi_d = 0.18$, [ferroin] $= 1.61 \times 10^{-5}$ M, and $T = 23$ °C[a]

j	D_{j1}	D_{j2}	D_{j3}
1	$(5 \pm 0.3) \times 10^{-7}$	$(5.2 \pm 2) \times 10^{-6}$	$(-4.5 \pm 1) \times 10^{-5}$
2	$(-1.2 \pm 0.2) \times 10^{-8}$	$(1.2 \pm 0.3) \times 10^{-6}$	$(-1.2 \pm 0.1) \times 10^{-5}$
3	$(2.2 \pm 3) \times 10^{-10}$	$(3.2 \pm 1) \times 10^{-9}$	$(4 \pm 0.7) \times 10^{-7}$

[a] Averaged values were found using the same procedure as for the system water(1)/AOT(2)/MA(3)/octane: $K_{1\_RID} = -2.05$ V/M, $K_{2\_RID} = 42.3$ V/M, $K_{3\_RID} = 554$ V/M, $K_{3\_spec} \equiv l_c\epsilon_{510} = 1.0 \times 10^4$ M^{-1}.

in which [AOT] or $[H_2O]$ in the injected sample differs from its value in the eluent, we actually change the radius R_w of water droplets, which depends on the ratio $[H_2O]/[AOT]$ as $R_w \cong 0.17\omega$. For small R_w ($\omega < 9$), all water molecules in a nanodroplet are bound and ϵ is small (around 10 or less), while for free water molecules in the center of a nanodroplet with $\omega > 10$, $\epsilon \cong 80$. Thus, experiments with $\omega_{in} > \omega_0$ (ω_0 here is ω in the eluent microemulsion; ω_{in} is ω in the injected sample) and with $\omega_{in} < \omega_0$ should have slightly different K_1 values. We, however, used in our calculations a constant value of K_1 ($= -2.07$ V/M).

The cross-diffusion coefficients D_{12} and D_{21} found in our experiments coincide well with those found previously.[22] Looking at Tables 4, 6, and 7, we can see that the absolute values of all coefficients D_{kl} for $l > k$ ($l < k$) are much larger (smaller) than the diagonal elements D_{kk} or D_{ll}. To understand qualitatively the results obtained, we are exploring the dependence of the water droplet radius on the concentrations of solutes as well as the following theoretical equations[26]

$$D_{kk} = D_k^* + c_k(\partial D_k^*/\partial c_k) \quad (59)$$

$$D_{kl} = c_k(\partial D_k^*/\partial c_l)(l \neq k) \quad (60)$$

where D_k^* is the intradiffusion coefficient, approximately equal in our case to the coefficient D_d of an entire droplet, and consequently all D_k^* are equal; c_k is the concentration of solute k (1 = H_2O, 2 = AOT, and 3 corresponds to one of the BZ reactants, MA or ferroin).

Consider first the coefficients D_{12} and D_{21}. If we increase c_2, the radius of a droplet R_w decreases and consequently (due to the Stokes−Einstein relation) D_d increases. Hence $\partial D_d/\partial c_2$ is positive and D_{12} should be positive. If we increase c_1, the radius of a droplet increases, D_d decreases, $\partial D_d/\partial c_1 < 0$ and D_{21} should be negative. The actual values of D_{12} and D_{21} follow from the dependences of the droplet radius on c_1 and c_2.[26]

With ferroin as the fourth component (c_3), we do not have an analytical expression for the dependence of R_w on [ferroin]. However, the DLS experiments indicate the emergence of clusters as [ferroin] increases. If ferroin is located in the surfactant layer (since phenanthroline is hydrophobic), it may deform the spherical droplets, leading to clustering or enlarging of R_w. Clustering implies that $\partial D_d/\partial c_3$ should be negative and consequently D_{13} and D_{23} also should be negative. Very large negative values of D_{13} and D_{23} may arise with large clusters (radius *ca.* 20 nm) or droplets containing ferroin.

In the case of malonic acid, we did not observe noticeable changes in the size of water droplets, and therefore the most plausible mechanism appears to be "excluded volume".[52,53] The larger concentration of MA induces a larger effective concentration of water in the droplet, since the volume available for motion of water inside the droplets, or, more precisely, in the aqueous pseudophase, becomes smaller. In the "excluded volume" mechanism, the cross-diffusion coefficients can be expressed as $D_{ik} \cong D_{ii}V_kc_i/(1 - \varphi_k)^2$, where V_k is the molar volume and $\varphi_k = V_kc_k$ is the volume fraction of malonic acid in the aqueous phase. This hypothesis, however, does not explain the cross-diffusion between MA and AOT, D_{23}. Perhaps a small decrease of the droplet radius with increasing [MA] also plays a role. More data, and especially the dependence of D_{13} and D_{23} on [MA], are needed.

It is difficult to characterize at this stage, without knowing the cross-diffusion coefficients for the other BZ reactants (especially Br^-, Br_2, and $HBrO_2$), what precise role cross-diffusion plays in pattern formation in the BZ−AOT system. It does seem clear, though, both from the experiments presented here and from preliminary calculations, that introduction of nonreactive neutral molecules like AOT and H_2O into the

reaction−diffusion equations can change the diffusion fluxes of reactive molecules through cross-diffusion and can consequently contribute significantly to the observed patterns.

If the large negative cross-diffusion coefficients D_{13} and D_{23} for ferroin are explained by an increase in the droplet radius or by clustering of small droplets promoted by ferroin molecules, then it seems plausible that in the BZ−AOT system all other molecules present inside water droplets have counterfluxes induced by the gradient of [ferroin] or [ferriin] (oxidized form of ferroin), i.e., negative cross-diffusion coefficients. This hypothesis can be used in simulating, for example, Turing patterns in the BZ−AOT system with the classical Oregonator model[54] with only three species ($HBrO_2$, Br^-, and catalyst) possessing nonzero cross-diffusion coefficients and nearly equal main diffusion coefficients.

Acknowledgment. We are grateful to Derek Leaist for practical advice and encouragement. This work was supported in part by the Chemistry Division of the National Science Foundation through grants CHE-0615507 and CHE-0625866 and by the donors of the American Chemical Society Petroleum Research Fund through grant 42222-AC6.

Appendix I. Derivation of eq 9

If we replace R by $R_0 r$, eqs 6–8 give

$$R_0^2\,\partial c_i/\partial t = R_0^2 D_{i1}\partial^2 c_1/\partial z^2 + R_0^2 D_{i2}\partial^2 c_2/\partial z^2 + R_0^2 D_{i3}\partial^2 c_3/\partial z^2 - (\partial c_i/\partial z)R_0^2 u_0(1-2r^2) + D_{i1}(\partial^2 c_1/\partial r^2 + r^{-1}\,\partial c_1/\partial r) + D_{i2}(\partial^2 c_2/\partial r^2 + r^{-1}\,\partial c_2/\partial r) + D_{i3}(\partial^2 c_3/\partial r^2 + r^{-1}\,\partial c_3/\partial r)(i=1,2,3) \quad \text{(A1.1)}$$

We assume that the terms $\partial^2 c_i/\partial z^2$ are small, i.e., $R_0{}^2\partial^2 c_i/\partial z^2 \ll \partial^2 c_i/\partial r^2 + r^{-1}\partial c_i/\partial r$ and/or $D_{ij}\partial^2 c_j/\partial z^2 \ll (\partial c_i/\partial z)u_0(1-2r^2)$ so that the first three terms on the right-hand side of eq A1.1 can be neglected. In effect, we ignore axial diffusion and take into account only radial diffusion in the flowing mixture. We further assume that at long times, i.e., far down the tube, the mixture has reached a steady state, so that $\partial c_i/\partial t = 0$. These two assumptions are independent of the number of components and were first introduced by Taylor for two-component systems [34] and then used by Price for three-component systems.[35] Price showed that these assumptions are valid if $L/u_0 \gg 2R_0{}^2/(3.8^2 D_{ii})$, where L is the distance from the injector to the detector.[35] In general, the diagonal elements D_{ii} should be replaced by the eigenvalues of matrix **D**, which are always real and positive, while D_{ii} can be negative.[55] The validity of these assumptions is also justified by accurate (1−3%) measurements of binary diffusion coefficients.[36] Under these assumptions, eq A1.1 can be written as

$$r_u\,\partial c_1/\partial z = D_{11}(\partial^2 c_1/\partial r^2 + r^{-1}\,\partial c_1/\partial r) + D_{12}(\partial^2 c_2/\partial r^2 + r^{-1}\,\partial c_2/\partial r) + D_{13}(\partial^2 c_3/\partial r^2 + r^{-1}\,\partial c_3/\partial r) \quad \text{(A1.2)}$$

$$r_u\,\partial c_2/\partial z = D_{21}(\partial^2 c_1/\partial r^2 + r^{-1}\,\partial c_1/\partial r) + D_{22}(\partial^2 c_2/\partial r^2 + r^{-1}\,\partial c_2/\partial r) + D_{23}(\partial^2 c_3/\partial r^2 + r^{-1}\,\partial c_3/\partial r) \quad \text{(A1.3)}$$

$$r_u\,\partial c_3/\partial z = D_{31}(\partial^2 c_1/\partial r^2 + r^{-1}\,\partial c_1/\partial r) + D_{32}(\partial^2 c_2/\partial r^2 + r^{-1}\,\partial c_2/\partial r) + D_{33}(\partial^2 c_3/\partial r^2 + r^{-1}\,\partial c_3/\partial r) \quad \text{(A1.4)}$$

where $r_u \equiv R_0{}^2 u_0(1-2r^2)$. Solving eq A1.4 for $\partial^2 c_3/\partial r^2 + r^{-1}\partial c_3/\partial r$ and substituting the result into eqs A1.2and A1.3 gives

$$r_u[\partial c_1/\partial z - (D_{13}/D_{33})\,\partial c_3/\partial z] = (D_{11} - D_{13}D_{31}/D_{33})(\partial^2 c_1/\partial r^2 + r^{-1}\,\partial c_1/\partial r) + (D_{12} - D_{13}D_{32}/D_{33})(\partial^2 c_2/\partial r^2 + r^{-1}\,\partial c_2/\partial r) \quad \text{(A1.5)}$$

$$r_u[\partial c_2/\partial z - (D_{23}/D_{33})\,\partial c_3/\partial z] = (D_{22} - D_{23}D_{32}/D_{33})(\partial^2 c_2/\partial r^2 + r^{-1}\,\partial c_2/\partial r) + (D_{21} - D_{23}D_{31}/D_{33})(\partial^2 c_1/\partial r^2 + r^{-1}\,\partial c_1/\partial r) \quad \text{(A1.6)}$$

Then, we can eliminate $(\partial^2 c_2/\partial r^2 + r^{-1}\partial c_2/\partial r)$ from eqs A1.5 and A1.6 to obtain

$$R_0^2 u_0(1-2r^2)[\det(\mathbf{M}_{D11})\,\partial c_1/\partial z - \det(\mathbf{M}_{D21})\,\partial c_2/\partial z + ([D_{23}\det(\mathbf{M}_{D21}) - D_{13}\det(\mathbf{M}_{D11})]/D_{33})\,\partial c_3/\partial z] = (\partial^2 c_1/\partial r^2 + r^{-1}\,\partial c_1/\partial r)[\det(\mathbf{M}_{D11})\det(\mathbf{M}_{D22}) - \det(\mathbf{M}_{D21})\det(\mathbf{M}_{D12})]/D_{33} \quad \text{(A1.7)}$$

Assuming that $\partial c_i/\partial z$ is independent of r, eq A1.7 has the solution:

$$c_1 = c_{1z} + T_1(r^2 - r^4/2) \quad \text{(A1.8)}$$

where

$$T_1 = (R_0^2 u_0/4)[D_{33}\det(\mathbf{M}_{D11})\,\partial c_1/\partial z - D_{33}\det(\mathbf{M}_{D21})\,\partial c_2/\partial z + ([D_{23}\det(\mathbf{M}_{D21}) - D_{13}\det(\mathbf{M}_{D11})])\,\partial c_3/\partial z]/[\det(\mathbf{M}_{D11})\det(\mathbf{M}_{D22}) - \det(\mathbf{M}_{D21})\det(\mathbf{M}_{D12})] \quad \text{(A1.9)}$$

The rate of transfer of c_1 across the cross-section of the tube is

$$Q_1 = 2\pi R_0^2 u_0 \int_0^1 r c_1(1-2r^2)dr \quad \text{(A1.10)}$$

Substituting c_1 from (A1.8) into (A1.10), we have

$$Q_1 = \text{constant} - 2\pi R_0^2 u_0 T_1/24 \quad \text{(A1.11)}$$

Applying the continuity equation, we can write that

$$\partial Q_1/\partial z = -\pi R_0^2\,\partial\langle c_1\rangle/\partial t \quad \text{(A1.12)}$$

where $\langle c_1\rangle$ is the average concentration c_1 over the cross-section of the tube. The condition of long time implies that the radial variation of c_1 is small, so that $\partial\langle c_1\rangle/\partial t \cong \partial c_1/\partial t$ at a fixed z.[35] Then, eqs A1.9, A1.11, and A1.12 give

$$(R_0^2 u_0^2/48)[\det(\mathbf{M}_{D11})\partial^2 c_1/\partial z^2 - \det(\mathbf{M}_{D21})\partial^2 c_2/\partial z^2 + \det(\mathbf{M}_{D31})\partial^2 c_3/\partial z^2]/\det(\mathbf{D}) = \partial c_1/\partial t \quad \text{(A1.13)}$$

since $D_{33}/[\det(\mathbf{M}_{D11})\det(\mathbf{M}_{D22}) - \det(\mathbf{M}_{D21})\det(\mathbf{M}_{D12})] = 1/\det(\mathbf{D})$ and $[D_{23}\det(\mathbf{M}_{D21}) - D_{13}\det(\mathbf{M}_{D11})] = D_{33}\det(\mathbf{M}_{D31})$. The coefficients in front of $\partial^2 c_1/\partial z^2$, $\partial^2 c_2/\partial z^2$, and $\partial^2 c_3/\partial z^2$ in (A1.13) are equal respectively to F_{11}, F_{12}, and F_{13} in eq 8. Equations analogous to A1.13 can be deduced from eqs A1.2–A1.4 for the concentrations c_2 and c_3, with respective coefficients F_{2j} and F_{3j}.

Appendix II. Derivation of eqs 24 and 26

Starting from eq 23, we can sum the experimental pre-exponential terms to get

$$\sum_{i=1}^{3} P_{i,\mathrm{exp}} = \sum_{j=1}^{3} K_j \sum_{i=1}^{3} B_{ji} \tag{A2.1}$$

Substituting eq 19, we have

$$\sum_{i=1}^{3} P_{i,\mathrm{exp}} = (\pi R_0^2)^{-1} \sum_{i=1}^{3} K_i P_i \tag{A2.2}$$

Using eqs $P_i = c_{i0}V_0$ and $\pi R_0^2/V_0 = l_0^{-1}$, A2.2 transforms to:

$$l_0^{-1} \sum_{i=1}^{3} P_{i,\mathrm{exp}} = \sum_{i=1}^{3} K_i c_{i0} \tag{A2.3}$$

which is eq 24.

To find a relation between the coefficients F_{ij} and the data obtained by fitting the experimental peaks (σ_i and $P_{i,\mathrm{exp}}$), we start again from eq 23. Multiplying $P_{i,\mathrm{exp}}$ by σ_i we get

$$\sigma_i P_{i,\mathrm{exp}} = \sigma_i \sum_{j=1}^{3} K_j B_{ji} \qquad i = 1, 2, 3 \tag{A2.4}$$

Summing over i in eq A2.4:

$$\sum_{i=1}^{3} \sigma_i P_{i,\mathrm{exp}} = \sum_{i=1}^{3} K_i \sum_{j=1}^{3} \sigma_j B_{ij} \tag{A2.5}$$

Inserting eq 14 into eq A2.5, we have

$$\sum_{i=1}^{3} \sigma_i P_{i,\mathrm{exp}} = \sum_{i=1}^{3} K_i \sum_{j=1}^{3} F_{ij} \sum_{k=1}^{3} B_{jk} \tag{A2.6}$$

Using eq 19 gives

$$(\pi R_0^2) \sum_{i=1}^{3} \sigma_i P_{i,\mathrm{exp}} = \sum_{i=1}^{3} K_i \sum_{j=1}^{3} P_j F_{ij} \tag{A2.7}$$

Finally, replacing P_j with $c_{j0}V_0$, we have:

$$l_0^{-1} \sum_{i=1}^{3} \sigma_i P_{i,\mathrm{exp}} = \sum_{j=1}^{3} c_{j0} \sum_{i=1}^{3} K_i F_{ij} \tag{A2.8}$$

which is eq 26.

Appendix III. Equations for the three-component system

The equations derived for the four-component system are applicable to the three-component system after appropriate modification. Equation 9 becomes

$$\frac{\partial c_i}{\partial t} = \sum_{j=1}^{2} E_{ij} \frac{\partial^2 c_j}{\partial z^2} \tag{A3.1}$$

where the matrix **E** is the counterpart of **F** for the three-component system. Equation 10 now becomes

$$E_{11} = K_{FD} D_{22}/\det(\mathbf{D_2}), E_{12} = -K_{FD} D_{21}/\det(\mathbf{D_2}),$$
$$E_{21} = -K_{FD} D_{12}/\det(\mathbf{D_2}), E_{22} = K_{FD} D_{11}/\det(\mathbf{D_2}) \tag{A3.2}$$

where $K_{\mathrm{FD}} \equiv R_0^2 u_0^2/48$ and $\det(\mathbf{D_2}) = D_{11}D_{22} - D_{12}D_{21}$.

The transformation from the coefficients E_{ij} to the coefficients D_{ij} (cf. eq 11) assumes the form

$$D_{11} = K_{FD} E_{22}/\det(\mathbf{E}), D_{12} = -K_{FD} E_{12}/\det(\mathbf{E}),$$
$$D_{21} = -K_{FD} E_{21}/\det(\mathbf{E}), D_{22} = K_{FD} E_{11}/\det(\mathbf{E}) \tag{A3.3}$$

where $\det(\mathbf{E}) = E_{11}E_{22} - E_{12}E_{21}$.

Equation 14 transforms into

$$s_j A_{ij} = \sum_{k=1}^{2} E_{ik} A_{kj} \qquad i = 1, 2; j = 1, 2 \tag{A3.4}$$

where the s_i are the eigenvalues of **E** and the A_{ij} are the counterparts of the B_{ij} for the three-component system.

The equations for the A_{ij} can be easily written, since they are much less cumbersome than the equations for the B_{ij}:

$$A_{11} = (\pi R_0^2)^{-1}[P_1(E_{11} - s_2) + P_2 E_{12}]/(s_1 - s_2) \tag{A3.5}$$

$$A_{12} = (\pi R_0^2)^{-1}[P_1 E_{12} E_{21}/(s_1 - E_{22}) - P_2 E_{12}]/(s_1 - s_2) \tag{A3.6}$$

$$A_{21} = (\pi R_0^2)^{-1}[P_2 E_{12} E_{21}/(s_2 - E_{11}) - P_1 E_{21}]/(s_2 - s_1) \tag{A3.7}$$

$$A_{22} = (\pi R_0^2)^{-1}[P_2(E_{22} - s_1) + P_1 E_{21}]/(s_2 - s_1) \tag{A3.8}$$

and the concentrations c_i are expressed as

$$c_i = A_{i1} G_1 + A_{i2} G_2 \qquad i = 1, 2 \tag{A3.9}$$

The general expression analogous to eq 24 for determining the sensitivity coefficients K_1 and K_2 (cf. eq 22) is

$$l_0^{-1}(P_{1,\mathrm{exp}} + P_{2,\mathrm{exp}}) = K_1 c_{10} + K_2 c_{20} \tag{A3.10}$$

From experiments involving injections with only $c_{i0} \neq 0$, we have

$$K_i = l_0^{-1}(P_{1,\mathrm{exp\_}i} + P_{2,\mathrm{exp\_}i})/c_{i0} \qquad i = 1, 2 \tag{A3.11}$$

Knowing K_1 and K_2, we can find the E_{ij} from the following four equations:

$$K_1 E_{11} + K_2 E_{21} = C_1 \tag{A3.12}$$

$$K_1 E_{12} + K_2 E_{22} = C_2 \tag{A3.13}$$

$$E_{11} + E_{22} = s_1 + s_2 \tag{A3.14}$$

$$E_{11}E_{22} - E_{12}E_{21} = s_1 s_2 \tag{A3.15}$$

where $C_i = l_0^{-1}[P_{1,\mathrm{exp\_}i} s_1 + P_{2,\mathrm{exp\_}i} s_2]/c_{i0}$, $i = 1, 2$. Equations A3.12–A3.15 are analogous to eqs 27–29 and follow from eq A3.16, which is analogous to the fundamental eq 26.

$$l_0^{-1}[P_{1,\mathrm{exp}} s_1 + P_{2,\mathrm{exp}} s_2] = (K_1 E_{11} + K_2 E_{21}) c_{10} + (K_1 E_{12} + K_2 E_{22}) c_{20} \tag{A3.16}$$

Solving eqs A3.12–A3.15 for E_{11}, we find

$$E_{11} = [s_1 s_2 + C_1 C_2/(K_1 K_2) - (s_1 + s_2) C_1/K_1]/(C_2/K_2 - C_1/K_1) \tag{A3.17}$$

The expressions for E_{12}, E_{21}, and E_{22} are straightforward.

In general, to determine the four E_{ij} it is sufficient to perform only two experiments, with $c_{20} = 0$ and $c_{10} = 0$. The measured dispersions s_i should be identical, i.e., $s_{1\_1} = s_{1\_2}$ and $s_{2\_1} = s_{2\_2}$, where the second subindex indicates the number of the experiment.

Supporting Information Available: Details of the calculation of the $\mathbf{B_{ij}}$ from the $\mathbf{F_{ij}}$ and a schematic drawing of the apparatus for the Taylor dispersion experiments. This material is available free of charge via the Internet at http://pubs.acs.org.

References and Notes

(1) Turing, A. M. *Philos. Trans. R. Soc. London. Ser. B* **1952**, *237*, 37–72.

(2) Koga, S.; Kuramoto, Y. *Prog. Theor. Phys.* **1980**, *63*, 106–121.
(3) Vanag, V. K.; Epstein, I. R. *Chaos* **2007**, *17*, 037110.
(4) Nicola, E. M.; Bar, M.; Engel, H. *Phys. Rev. E* **2006**, *73*, 066225.
(5) Vanag, V. K.; Epstein, I. R. *Phys. Rev. Lett.* **2002**, *88*, 088303.
(6) Zhabotinsky, A. M.; Dolnik, M.; Epstein, I. R. *J. Chem. Phys.* **1995**, *103*, 10306–10314.
(7) Vastano, J. A.; Pearson, J. E.; Horsthemke, W.; Swinney, H. L. *Phys. Lett. A* **1987**, *124*, 320–324.
(8) Abdusalam, H. A.; Fahmy, E. S. *Chaos Solitons & Fractals* **2003**, *18*, 259–266.
(9) del Castillo-Negrete, D.; Carreras, B. A.; Lynch, V. *Physica D* **2002**, *168*, 45–60.
(10) Roussel, C. J.; Roussel, M. R. *Prog. Biophys. Mol. Biol.* **2004**, *86*, 113–160.
(11) Roussel, M. R.; Wang, J. *Phys. Rev. Lett.* **2001**, *87*, 188302.
(12) Vasilev, V. A.; Romanovsky, Ju. M.; Yakhno, V. G. *Autowave Processes*; Nauka: Moscow, 1987.
(13) Andersen, P.; Bache, M.; Mosekilde, E.; Dewel, G.; Borckmans, P. *Phys. Rev. E* **1999**, *60*, 297–301.
(14) Budrene, E. O.; Berg, H. C. *Nature* **1995**, *376*, 49–53.
(15) Woodward, D. E.; Tyson, R.; Myerscough, M. R.; Murray, J. D.; Budrene, E. O.; Berg, H. C. *Biophys. J.* **1995**, *68*, 2181–2189.
(16) Budrene, E. O.; Berg, H. C. *Nature* **1991**, *349*, 630–633.
(17) Polezhaev, A. A.; Pashkov, R. A.; Lobanov, A. I.; Petrov, I. B. *Int. J. Develop. Biol.* **2006**, *50*, 309–314.
(18) MacEwan, K.; Leaist, D. G. *J. Phys. Chem. B* **2002**, *106*, 10296–10300.
(19) Epstein, I. R.; Vanag, V. K. *Chaos* **2005**, *15*, 047510.
(20) Vanag, V. K. *Phys. Usp.* **2004**, *47*, 923–941.
(21) Vanag, V. K.; Epstein, I. R. In *Self-Organized Morphology in Nanostructured Materials*; Al-Shamery, K., Parisi, J., Eds.; Springer: Berlin, 2008; pp 89−113.
(22) Leaist, D. G.; Hao, L. *J. Phys. Chem.* **1995**, *99*, 12896–12901.
(23) Costantino, L.; Dellavolpe, C.; Ortona, O.; Vitagliano, V. *J. Chem. Soc., Faraday Trans.* **1992**, *88*, 61–63.
(24) Costantino, L.; Dellavolpe, C.; Ortona, O.; Vitagliano, V. *J. Colloid Interface Sci.* **1992**, *148*, 72–79.
(25) Kotlarchyk, M.; Chen, S. H.; Huang, J. S. *J. Phys. Chem.* **1982**, *86*, 3273–3276.
(26) Leaist, D. G. *Phys. Chem. Chem. Phys.* **2002**, *4*, 4732–4739.
(27) Tyrrell, H. J. V.; Harris, K. R. *Diffusion in Liquids: A theoretical and experimental study*; Butterworths: London, 1984.
(28) Cussler, E. L.; Dunlop, P. J. *J. Phys. Chem.* **1966**, *70*, 1880–1888.
(29) Annunziata, O.; Vergara, A.; Paduano, L.; Sartorio, R.; Miller, D. G.; Albright, J. G. *J. Phys. Chem. B* **2003**, *107*, 6590–6597.
(30) Gosting, L. J.; Kim, H.; Loewenst, M. A.; Reinfeld, G.; Revzin, A. *Rev. Sci. Instrum.* **1973**, *44*, 1602–1609.
(31) Leaist, D. G. *J. Chem. Soc., Faraday Trans. 1* **1987**, *83*, 829–839.
(32) Noulty, R. A.; Leaist, D. G. *J. Phys. Chem.* **1987**, *91*, 1655–1658.
(33) Rai, G. P.; Cullinan, H. T. *J. Chem. Eng. Data* **1973**, *18*, 213–214.
(34) Taylor, G. I. *Proc. R. Soc. London Ser. A* **1953**, *219*, 186–203.
(35) Price, W. E. *J. Chem. Soc., Faraday Trans. 1* **1988**, *84*, 2431–2439.
(36) Alizadeh, A.; DeCastrro, C. A. N.; Wakeham, W. A. *Int. J. Thermophys.* **1980**, *1*, 243–284.
(37) MacEwan, K.; Leaist, D. G. *Phys. Chem. Chem. Phys.* **2003**, *5*, 3951–3958.
(38) Leaist, D. G. *Ber. Bunsen-Ges.* **1991**, *95*, 117–122.
(39) Kim, H. *J. Phys. Chem.* **1969**, *73*, 1716–1722.
(40) Kim, H. *J. Phys. Chem.* **1966**, *70*, 562.
(41) Fletcher, P. D. I.; Howe, A. M.; Robinson, B. H. *J. Chem. Soc., Faraday Trans. 1* **1987**, *83*, 985–1006.
(42) Ray, S.; Bisal, S. R.; Moulik, S. P. *J. Chem. Soc., Faraday Trans.* **1993**, *89*, 3277–3282.
(43) Gill, P. E.; Murray, W. *SIAM J. Numer. Anal.* **1978**, *15*, 977–992.
(44) Alizadeh, A.; Wakeham, W. A. *Int. J. Thermophys.* **1982**, *3*, 307.
(45) Dunlop, P. J. *J. Phys. Chem.* **1965**, *69*, 4276–4283.
(46) D'Angelo, M.; Fioretto, D.; Onori, G.; Santucci, A. *Phys. Rev. E* **1998**, *58*, 7657–7663.
(47) Feldman, Y.; Kozlovich, N.; Nir, I.; Garti, N. *Phys. Rev. E* **1995**, *51*, 478–491.
(48) Ponton, A.; Bose, T. K.; Delbos, G. *J. Chem. Phys.* **1991**, *94*, 6879–6886.
(49) Bardow, A.; Goke, V.; Koss, H. J.; Marquardt, W. *AIChE J.* **2006**, *52*, 4004–4015.
(50) D'Angelo, M.; Fioretto, D.; Onori, G.; Palmieri, L.; Santucci, A. *Phys. Rev. E* **1996**, *54*, 993–996.
(51) Mittleman, D. M.; Nuss, M. C.; Colvin, V. L. *Chem. Phys. Lett.* **1997**, *275*, 332–338.
(52) Capuano, F.; Vergara, A.; Paduano, L.; Annunziata, O.; Sartorio, R. *J. Phys. Chem. B* **2003**, *107*, 12363–12369.
(53) Jakupi, P.; Halvorsen, H.; Leaist, D. G. *J. Phys. Chem. B* **2004**, *108*, 7978–7985.
(54) Field, R. J.; Noyes, R. M. *J. Chem. Phys.* **1974**, *60*, 1877–1884.
(55) Miller, D. G.; Vitagliano, V.; Sartorio, R. *J. Phys. Chem.* **1986**, *90*, 1509–1519.

JP800525W